



Experimental and numerical studies on the flexural behaviour of GFRP laminated hybrid-fibre-reinforced concrete (HFRC) beams

B. Ramesh¹ · S. Eswari¹ · T. Sundararajan¹

Received: 18 April 2020 / Accepted: 19 September 2020 / Published online: 12 October 2020
© Springer Nature Switzerland AG 2020

Abstract

The main objective of this paper is to study the structural behaviour of hybrid fibre-reinforced concrete beams strengthened with glass fibre-reinforced polymer (GFRP) laminates. For the above purpose, three distinct groups of beam elements were cast, namely: (1) group A consisting of reinforced concrete (RC) and laminated RC beams, (2) group B consisting of fibre-reinforced concrete (FRC) and laminated FRC beams and (3) group C consisting of hybrid fibre-reinforced concrete (HFRC) and laminated HFRC beams. In beams of group B, basalt fibres were incorporated with a total volume fraction of 1%, whereas in group C beams, polyolefin and basalt fibres in the ratio of 30:70 were used with the total volume fraction of 1%. For lamination, 5-mm-thick GFRP sheet was used at the soffit of the all laminated beams. All the beams were tested under the four-point bending, until failure. The study parameters included evaluation of initial crack load, yield load and ultimate load and their corresponding deflections, ductility and failure modes. From the results, it was observed that the laminated HFRC beams exhibited higher load carrying capacity and larger deformation than the other beams. The ultimate load of laminated RC beam was about 33.44% higher than that of the control beams. The ultimate load of laminated HFRC improved by about 83.04% and 37.16% than the control and laminated RC beam, respectively. The load at FRP debonding initiation for ‘laminated HFRC beam’ is 43.06% higher than the laminated RC beam and 10.34% higher than the ‘laminated FRC beam’. Moreover, a 3-D finite element (FE) technique was adopted to simulate the performance of the beam elements. A fairly similar agreement was reached between the findings of the experimental and FE model results.

Keywords Basalt fibres · FRC · FE model · Flexure · GFRP · HFRC · Polyolefin fibres · Ductility

Introduction

Need for strengthening of reinforced concrete (RC) structures is becoming more apparent, particularly, when there is an enhancement in peak load, a change in use, degradation problem and some design and/or construction deficiency. Use of externally bonded fibre-reinforced polymer (FRP) sheets/plates/strips/warps is a modern and easy way to strengthen RC beams [1, 2]. Several studies have stated that FRP composites when applied to RC members improve

the performance, durability and cost-effectiveness in rehabilitation [3–5]. Among the all fibres, glass fibres have high-temperature resistance, high strength and low cost, which makes glass fibre-reinforced polymer (GFRP) the most suitable FRP reinforcement for various civil engineering applications [6, 7]. Many researchers have reported that FRP-strengthened RC beams exhibit an increase in strength and decrease in ductility [8–10]. For successful strengthening, adequate bond between the FRP laminates and existing concrete members is a significant factor, whereas others reported that damage of interfacial bond due to ‘concrete cracking’ played a more important role [11, 12]. On the other hand, incorporating fibres in concrete effectively controls the crack development [13].

In order to solve the above problems, an effective approach is to include short discrete fibres into cement-based materials to increase its structural integrity. Addition of such fibres not only enhances the requisite properties of RC, but also changes the characteristics of the material from

✉ B. Ramesh
bramesh0104@pec.edu

S. Eswari
eswaripec@pec.edu

T. Sundararajan
tsrajan_56@pec.edu

¹ Department of Civil Engineering, Pondicherry Engineering College, Pondicherry 605 014, India

brittle to ductile [14, 15] and improves fatigue performance [16, 17]. A variety of fibres are existing such as natural, synthetic, steel and glass fibres [18, 19]. Steel fibre has high toughness and tensile strength [20], but workability reduction due to balling and corrosion are the key challenges in steel FRC [21]. Though glass fibre improves the concrete toughness, long-term strength of concrete is reduced due to alkali attack. High strength, chemically inert carbon fibres have a disadvantage of high cost. Advanced materials offer the assurance of innovative applications in concrete composite. Basalt fibre (BF) is an inorganic fibre which is derived from the molten basalt rock. The processing method of this type of fibre is like glass fibre, but less energy is used and no supplement is required, which makes it cheaper than carbon or glass fibres [22, 23]. The inclusion of basalt fibre extensively increases the energy absorption capacity and deformation of geo-polymer concrete [24]. It also enhances the tensile strength, fracture energy and flexural strength [25, 26].

The new synthetic polyolefin fibre, which is ductile and more flexible, is expected to improve strain capacity and toughness. Addition of polyolefin fibres improves the fracture energy, tensile strength [27] and restrains the shrinkage cracking in concrete [28]. It has been shown recently that HFRC composites can offer more desirable engineering properties than single FRC [29]. The flexural capacities of strengthened beam elements have also been investigated by the introduction of finite element (FE) modelling technique [30–33].

On the basis of a comprehensive literature review reported on the RC beam strengthening, external attachment of FRP lamination is found to be more effective. However,



the use of fibres and external strengthening in combination is uncommon. Therefore, studies which focus on both the strength and ductility of structural members are required to be undertaken. Hence, the key of this research is to assess the performance of GFRP strengthened RC beams along with the addition of polyolefin and basalt fibres. The purpose is to study the ductility and strength parameters of RC beams strengthened with HFRC and compare the same with the RC strengthened beam and control beam. Additionally, finite element models were developed using ANSYS software (version 15) for simulating the observed experimental behaviour.

Experimental study

Materials

OPC 53 grade was used; coarse aggregate and fine aggregate having a specific gravity of 2.63 and 2.63 and maximum size of 20 and 4.75 mm were used in this study. Throughout the study, tap water was used for manufacturing concrete. A commercial superplasticizer (SP) ‘classic super flow’ conforming to IS: 9103-1999 [34], with the dosage of 0.5–1.5% by weight of cement, was used to enhance the concrete workability. In order to fabricate workable concrete, a water/cement (w/c) ratio of 0.46 has been used in this study [35]. Both basalt and polyolefin fibres, acquired from commercial establishments, were used in concrete. In the present study, two fibres were used to form the hybrid fibres. The properties of above-mentioned fibres are presented in Table 1.

Table 1 Salient properties of basalt and polyolefin fibres

Fibre(s)	Length (mm)	Diameter/thickness (mm)	Aspect ratio	Density (kg/m ³)	Young's modulus (GPa)	Tensile strength (MPa)
 Basalt fibre	18	1	18	2750	79.3–93.1	4500
 Polyolefin fibre	48	1.22	39.34	920	6.0–6.1	550

The longitudinal reinforcement for all the beams consisted of high yield strength deformed (HYSD) bars of 10 mm and 8 mm diameters, conforming to the relevant IS code. Commercially available unidirectional GFRP laminates were used for flexural strengthening of beams on the tension side. The GFRP coupons were prepared using the wet (hand) layup system as per ASTM [36]. The rupture strain and tensile strength of GFRP fabric determined from wet layup specimens were found to be 1.15% and 1300 MPa, respectively. Two-part epoxy resin (mixing ratio of resin to hardener = 4:1 by weight) was used, for bonding the laminates to the beams.

Mix proportioning and casting of beams

The proportioning of the concrete mixture has been carried out in accordance with IS: 10262-2009 [37], with a 31.6 MPa target mean strength, and this formed the ‘control mix’. The proportions of the control concrete mixture are given in Table 2. Basalt fibre with 1% fibre volume fraction (V_f) was incorporated into ‘control mix’ for casting fibre-reinforced concrete (FRC) beam specimens. Basalt along with polyolefin fibres has been mixed in the ratio of 70:30 at 1% fibre volume fraction (V_f) and incorporated into control mix for casting hybrid fibre-reinforced concrete (HFRC) beams. Three groups of RC beams were casted, which were

Table 2 The proportions of the control concrete

Cement (kg/m ³)	Water (kg/m ³)	Fine aggregates (kg/m ³)	Coarse aggregates (kg/m ³)	Water/cement ratio
389	181	761	1096	0.47

ordinary RC beams (B0P0 L0 and B0P0 L5) in group A, basalt FRC beams (B100P0 L0 and B100P0 L5) in group B, whereas the beams in group C were basalt and polyolefin HFRC beams (B70P30 L0 and B70P30 L5). In each group, a beam was strengthened using externally bonded unidirectional GFRP laminates (B0P0 L5, B100P0 L5 and B70P30 L5). The test program was aimed to examine the strength and deflection behaviour of RC, FRC and HFRC beams with and without laminates. All the beams had a size of 150 mm depth, 100 mm width and 1000 mm length. All beams were built in compliance with IS 456:2000 [38]. The reinforcement, dimension and geometry details of tested beams are shown in Fig. 1. The details of designation of beams are summarized in Table 3.

FRP strengthening of beams

All the beams were casted and then cured for 28 days, and after that, the strengthening process was carried out on the tension face of the beams using the ‘wet layup’ system in

Table 3 The designation and details of various beams

Group	Beam ID	Fibre volume fraction (%)	Proportion of fibres (%)		Thickness of GFRP laminate (mm)
			Basalt	Polyolefin	
A	B0P0 L0	0	0	0	0
	B0P0 L5	0	0	0	5
B	B100P0 L0	1.0	100	0	0
	B100P0 L5	1.0	100	0	5
C	B70P30 L0	1.0	70	30	0
	B70P30 L5	1.0	70	30	5

$V_f = 1.0\%$ (kept constant)

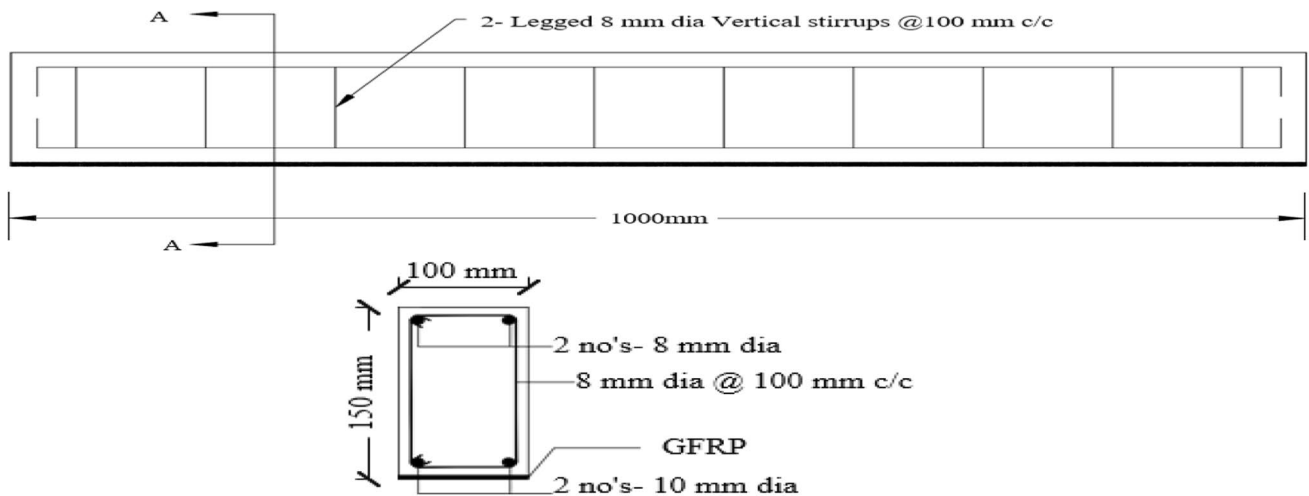


Fig. 1 Reinforcement details of beam

accordance with the American Concrete Institute specifications 440.2R-2008 [1]. Before bonding the laminates, the tension surface of all the beams was cleaned, dried and greased with contaminates, if any, removed. The tension side of the beams was prepared to a minimum rough profile (CSP 3) as defined in International Concrete Repair Institutes guidelines, (ICRI 03730) [39]. Abrasion disc was used to remove any loose cement paste layer such that one could see clearly the exposed aggregate particles. The various stages of preparation of surface are shown in Fig. 2.

The prepared surface was then uniformly coated with a primer and allowed to cure. After that, the resin and hardener were mixed in the predetermined ratio 4:1 with the mixing carried out according to the manufacture's recommendations, until a uniform colour was attained. The reinforcing glass fibres were cut according to the required size, cleaned to remove grease or contaminates, if any, present on the fibres. The epoxy resin was applied uniformly onto the prepared surface, and then, the reinforcing glass fibres were pressed onto the above surface with gentle pressure being applied using a rubber roller. This was done to make sure that the FRP sticks well to the surface, ensure expelling of entrapped air and to remove excessive epoxy that may be present between the FRP and concrete surface. Laminated beams thus prepared were cured for a week before testing them. The procedure for beam strengthening is shown in Fig. 2a–d.

Test set-up and instrumentation

All beams have been tested on a universal testing machine (UTM) available in the Department of Civil Engineering, PEC. The beams were simply supported with 50 mm offset from both the supports, having an effective span of 900 mm. Loads were applied with an increment of 2.5 kN under the four-point method. The load from the load cell was transferred to the beam with the help of a steel I-section spreader-beam. This load from the spreader beam got transferred onto the two loading points on the beam. A mechanical dial gauge having an accuracy of 0.01 mm was used to measure the deflections at the mid-span of beams, and crack-widths were measured using a crack detection microscope having a least count of 0.02 mm. Figure 3 shows the photographic view of the test set-up along with the instrumentation used. The loads were gradually increased until failure of the beams. Load and maximum deflection were recorded at each load interval. Further, crack propagation and distribution were marked and noted at every 10-kN loading interval. Load (in kN) and deflections (in mm) formed the basic experimental data, based on which load–deflection curves for all the beams were developed, and the ductility ratios were calculated to evaluate the relative ductility performance of the various beams.

Fig. 2 Step-by-step procedure for strengthening of beams: **a** Surface preparation, **b** GFRP fabric cutting, **c** application of epoxy on concrete surface, **d** squeezing out of entrapped air bubbles

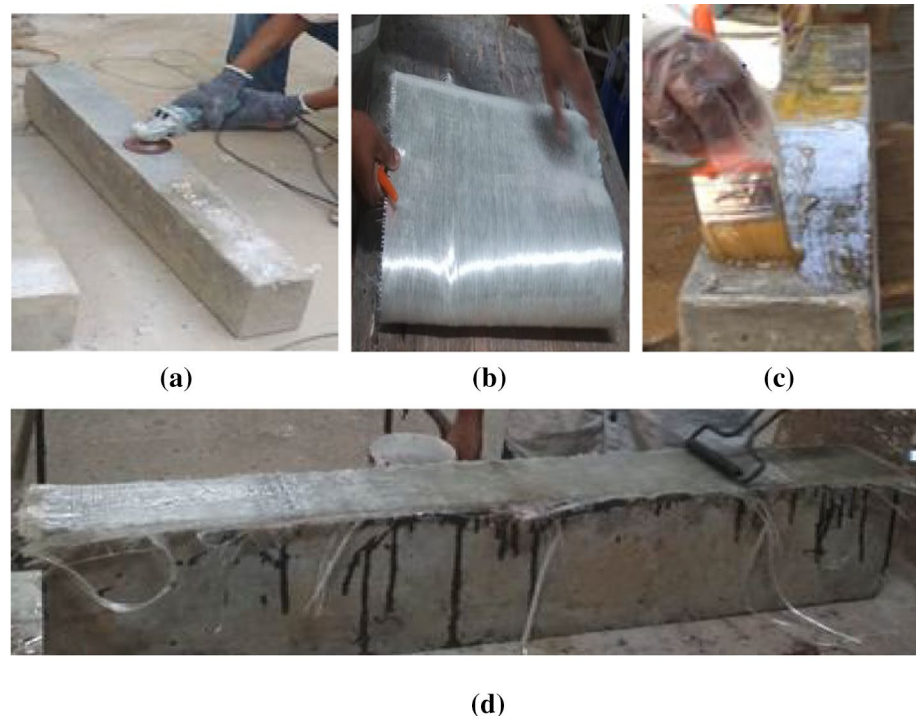


Fig. 3 The experimental test set-up



Components: 1. Load cell, 2. Spreader beam, 3. RC beam, 4. Supports, 5. Dial gauge

Experimental results and discussion

Effect on load carrying capacity

The experimental outcomes are shown in Table 4, in terms of the measured ultimate load, yield load and primary crack load and their corresponding deflections. The enhancement in the load carrying capacity of ‘laminated RC beam’ over the control beam at the above three stages was 31.1%, 41.2% and 33.4%, respectively. It shows that there is an effect of lamination on the strengthened beam at all the above three stages with the increase being very high at the first crack and ultimate stage, the highest being at the ultimate stage. Comparing the loads at the three stages of ‘laminated FRC beam’ with that of ‘laminated RC beam’, it was found that the percentage increase of loads was 9.86%, 27.6% and 27.7%. This shows the significant role played by adding basalt fibres in the strength enhancement of ‘laminated RC beam’. Comparing the ultimate, yield and first crack loads of ‘laminated HFRC beam’ with respect to that of ‘control beam’, the percentage increase is 79.13%, 108.82% and 81.86%, respectively. This shows that there is a ‘combined effect’ of fibres which extensively influences the above loads of ‘laminated HFRC beams’. Similar findings were observed by Syed et al. [40], Ramesh et al. [41, 42]. Figure 4 shows the load comparisons at various stages of tested beams.

Effect on deflection

The recorded deflections for all tested beams are listed in Table 4. The deflection at first crack, yield and at ultimate

stages recorded for control beam was 1.25 mm, 3.61 mm and 8.6 mm. The maximum deflection at all above three stages for ‘laminated RC beam’ was 1.30 mm, 3.76 mm and 6.3 mm, respectively. The deflection at all stages of ‘laminated RC beam’ decreases over the ‘control beam’ which indicates the contribution of stiffness due to laminates. Using basalt and polyolefin fibres for ‘laminated HFRC beams’ led to an increase in the deflections. The maximum percentage increase in the deflection at primary crack, yield and ultimate stages of ‘laminated HFRC’ beams over the ‘control beam’ is about 96%, 38.5% and 46.51%, respectively. Further, the increase in deflection at all above three stages of ‘laminated HFRC’ over the ‘laminated RC beam’ is about 88%, 32.97% and 100% respectively. This indicates that there is a ‘combined effect’ of fibres. Deflection at ultimate stage for laminated HFRC beam was found to be 16.33% less when compared to HFRC beam.

Effect on ductility

The ductility is a measurement of the capacity of the structural member to absorb energy and can be expressed as deformity resistance when transforming from the elastic to the plastic zone and failure. Ductility in a reinforced concrete member can be measured by using any of the following methods: (1) rotational ductility index, (2) curvature ductility index or (3) deflection ductility index. In the present study, ductility is calculated using deflection ductility index method. Deflection-based ductility (D_{Δ}) is defined as the ratio between ultimate deflection (Δ_u) to deflection during yield stage (Δ_y) [43]. That is,

Table 4 Experimental results of various tested beams

Group	Beam ID	First crack load (kN)	First crack deflection (mm)	Yield load (kN)	Yield deflection (mm)	Load at Initiation of debonding (kN)	Deflection at initiation of debonding (mm)	Crack width (mm)	Ultimate load (kN)	Ultimate deflection (mm)
A	B0P0 L0	17.54	1.25	34.00	3.61	-	42.34	-	08.60	0.76
	B0P0 L5	23.00	1.30	48.00	3.76	51.29	4.24	56.51	06.30	0.72
B	B100P0 L0	18.14	1.58	42.18	4.31	-	48.10	-	11.02	0.67
	B100P0 L5	25.27	1.81	61.25	4.57	66.5	4.62	72.15	09.56	0.59
C	B70P30 L0	24.41	2.27	53.00	4.71	-	61.19	-	15.06	0.63
	B70P30 L5	31.42	2.45	71.00	5.00	73.38	5.84	77.51	12.60	0.56

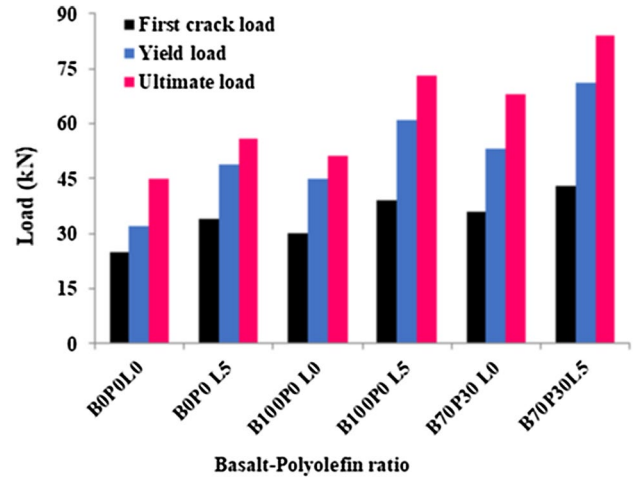


Fig. 4 Comparisons of loads at various stages

Table 5 Ductility indices of beams

SI no.	Beam ID	Deflection ductility (D_{Δ})	Energy ductility (D_E)
1	B0P0 L0	2.37	2.71
2	B0P0 L5	1.67	1.97
3	B100P0 L0	2.56	2.92
4	B100P0 L5	2.09	2.46
5	B70P30 L0	3.19	3.69
6	B70P30 L5	2.62	2.95

$$D_{\Delta} = \Delta_u / \Delta_y \tag{1}$$

Camata et al. [44] suggested the ductility in terms of energy (D_E). It is defined as the energy (area under load–deflection curve) of the beam at ultimate stage (E_u) divided by the energy of the beam at yield stage (E_y). That is,

$$D_E = E_u / E_y \tag{2}$$

The measured ductility in terms of energy and deflection is shown in Table 5 and Fig. 5

After examining the outcomes, it can be observed that the deflection and energy ductility were maximum for ‘HFRC beam’ [B70P30 L0]. As seen in Table 5, the deflection ductility dropped from 2.38 to 1.67 for control beam when compared to laminated RC beam. This indicates that a greater reduction in the ductility of the beam occurs when the beam is strengthened with GFRP laminates as is an external attachment to the RC beams and decreases the potential of redistribution of moments in the hogging region. Similar findings were reported by

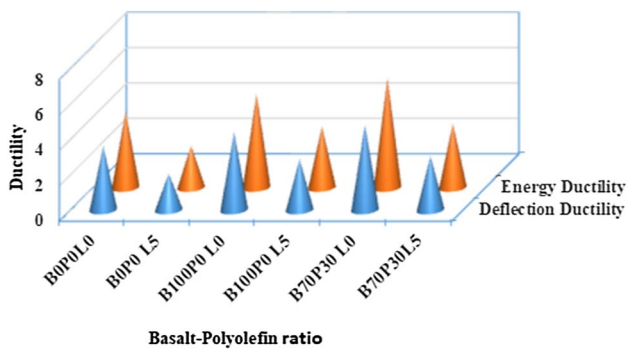


Fig. 5 Comparison of ductility of beams

Attari et al. [45], Jason duic [46]. Using ‘laminated RC’ sample as a reference beam, the deflection and energy ductility were enhanced by 25.14% and 56.88% and 24.87% and 49.74% for ‘laminated FRC’ and ‘laminated HFRC’ beams, respectively. This shows that there is a combined effect, which extensively enhances the ductility ratios of laminated HFRC beam.

Finite element analysis (FEA)

FEA software ANSYS (version 15) was used to model all the beams.

Element type

Selection of element type is more important in any FEA. The following elements were selected for modelling the beams.

Concrete Concrete was modelled using the 3-D ‘SOLID65’ element, which is defined by 8 nodes having 3 degree of freedom (DOF) at each node as shown in Fig. 6a. This element is capable of handling plastic deformation and cracking.

Steel reinforcement The longitudinal and transverse reinforcements were modelled using the two nodes ‘link180’ spar element with three DOF, i.e. translations at each node, as shown in Fig. 6b.

Steel Plates To model the steel plates at the point of application of load and at supports, ‘solid185 structural’ element was used (Fig. 6c).

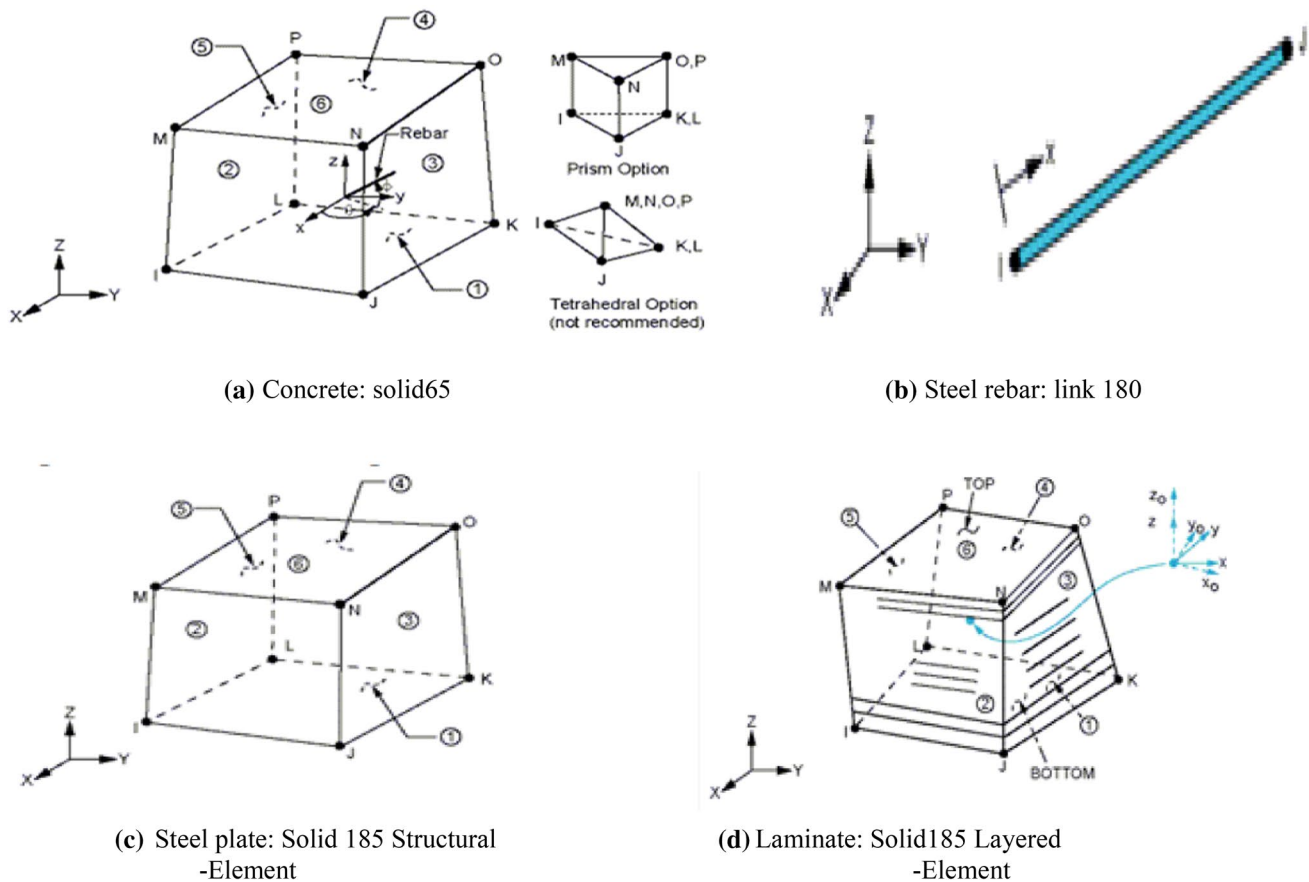


Fig. 6 a–d Details of the type of elements used for modelling of various components of beams [49]

GFRP laminates The GFRP laminates used for beam strengthening were modelled using ‘solid185-layered’ element, which has eight nodes and three DOF, i.e. translations (Fig. 6d). The connection between the concrete and GFRP was modelled using the (basic) concept that ‘the bond between the concrete and FRP is considered perfect’. The perfectly bonded model has been widely adopted by many researchers such as Hassan et al. [47], Jayajothi et al. [48].

Real constants

Real constants are properties that depended on the cross-sectional properties and the element type. Not all materials require elements of the same type and real constants may have different values. ‘Real constant set 26’ was used for the solid 65 elements. Values were entered for the volume ratio and material number. Values for cross-sectional (C/S) area and initial strain were entered. Zero strain value was adopted at the starting of the experiment because there is no primary stress in the beam. C/S area in sets 8 and 10 refers to the reinforcement of 8 mm (main) and 10 mm (hanger) diameter bars, respectively.

Material properties

Concrete is a brittle material, which exhibits a nonlinear behaviour both in compression and tension. The material properties used for plain concrete model are as follows: elastic modulus = 28062 MPa, Poisson’s ratio = 0.33, compressive strength = 33.23 MPa. Steel reinforcement for the model was assumed to exhibit an ‘elasto-plastic’ behaviour which is identical both in compression and tension. The modulus of elasticity, yield stress and Poisson’s ratio for steel were taken as 200,000 MPa, 415 MPa and 0.3, respectively. The behaviour of the GFRP materials was considered to be linear elastic up to failure, and the modulus of elasticity and tensile stress were considered as 1620 MPa, 515 MPa, respectively.

Modelling and gluing

Solid blocks were used to model concrete beam, supporting steel plates and GFRP laminate, while line elements were used to model steel reinforcement. ‘Glue’ command was used to attach the GFRP layer with the concrete beam.

Boundary conditions

Boundary conditions were applied at the loading points and supports. For all beams, the supports were modelled as simply supported, and the loading was applied using the four-point method. At the supports, displacements in all directions were constrained in the model to get a unique

solution. To simulate simply support condition, X, Y and Z directions at the nodes of one support were given constant values of zero. Similarly, only Y direction at the nodes of the other support was given a zero value. The beams were coupled at one-third of effective span, and two equal forces were applied on the coupled nodes.

Meshing

After developing the beam models with supporting plates, it has to be meshed before carrying out the process of analysis. Mesh tool which is available in preprocessor helps to establish mesh attributes, size control and mesh shape which are used for meshing the solid models. No reinforcement mesh is required because individual elements have been generated via the nodes in the modelling process. The GFRP laminates were meshed as brick elements. Square shape mesh of size 25 mm was chosen for all beams. Solution controls command was utilized to run the static analysis of all beams. The detail of overall meshing with boundary conditions for RC beam is shown in Fig. 7.

Comparison of experimental and numerical results of various beams

Experimental outcomes have been compared with FE model analysis. Comparisons were partial to main characteristics of beams such as primary crack, yield load, ultimate load, deflection and load–deflection response. Tables 6 and 7 summarize the load carrying capacity and their corresponding deflections at all above three stages of the various beams, acquired from the evolved FE models and experiments. The FE models results for loads are within $\pm 12\%$, and the deflections are within $\pm 8\%$ of the experimental results. This variation may be due to the reason that there is ‘perfect bond between the steel reinforcing and concrete’ as is assumed in the FE modelling, but this assumption is not true for the experimentally tested beams. The percentage difference is considerably reasonable and acceptable; similar observations were made by Choobbor et al. [33].

Load–deflection relationship

The developed finite element model (FEM) of full-scale beams results was compared with the outcomes obtained from the experimental investigations. Figure 8a–f shows the numerical and tested load–deflection response of beams at all loading stages. From the graph, it is observed that the first crack occurs at the linear region. Beyond that the curve becomes nonlinear and the yielding of steel takes place in this region with the failure occurring at the ultimate stage. The typical nodal displacement of beams at ultimate stage

Fig. 7 Typical FE modelling of RC beam

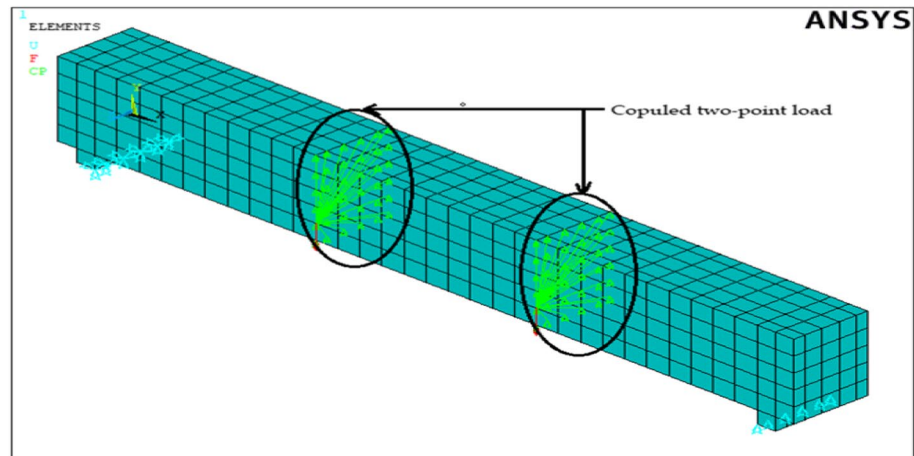


Table 6 Comparison of loads at various stages: experimental versus numerical

SI no.	Beam ID	First crack load(kN)		Yield load (kN)		Ultimate load (kN)	
		Experimental	Numerical	Experimental	Numerical	Experimental	Numerical
1	B0P0 L0	25.13	31.75	38.12	37.20	45.23	50.20
2	B0P0 L5	34.26	42.75	49.38	67.50	56.00	63.50
3	B100P0 L0	30.14	36.75	42.18	51.20	51.10	60.20
4	B100P0 L5	39.27	39.95	61.25	71.25	73.15	78.25
5	B70P30 L0	36.41	41.26	53.00	42.18	68.19	70.08
6	B70P30 L5	43.20	48.49	71.26	47.26	84.34	86.29

Table 7 Comparison of deflections at various stages: experimental versus numerical

SI no.	Beam ID	First crack deflection (mm)		Yield deflection (mm)		Ultimate deflection (mm)	
		Experimental	Numerical	Experimental	Numerical	Experimental	Numerical
1	B0P0 L0	0.55	0.23	2.21	1.46	08.03	07.24
2	B0P0 L5	0.26	0.11	2.34	1.10	04.86	04.26
3	B100P0 L0	0.38	0.27	2.50	1.66	11.02	10.34
4	B100P0 L5	0.19	0.14	3.31	1.92	09.56	07.42
5	B70P30 L0	0.42	0.32	3.12	2.19	15.06	12.38
6	B70P30 L5	0.39	0.29	4.22	1.86	12.92	08.97

is shown in Figs. 9 and 10. It is clear from Fig. 8a–f and Tables 6 and 7 that the load–deflection response of all beams from FE model analysis agrees well with the experimental results.

Delamination behaviour and cracking pattern

The crack pattern obtained from the FE modelling at each load step is compared with the tested beams. Figures 11 and 12 show the typical crack pattern of the tested and modelled beams. The control beam had initial flexural cracking accompanied by the concrete crushing in compression. The crack pattern for ‘laminated RC’ beams was observed by the development of vertical cracks at

the mid-span in the tension zone. With applying further loads, a greater number of diagonal cracks appeared and the initial cracks propagated towards the loading points. At the ultimate load, due to the sliding between the laminate and concrete, development of horizontal cracks in the tension zone was observed. This beam had a greater load carrying capacity as compared to the reference beam specimen, but brittle failure occurred due to debonding of laminates with a sudden decrease in load carrying capacity. More number of cracks was observed in laminated HFRC beam compared to the control and RC beam. Incorporation of fibres in concrete increased the load carrying capacity, resulting in ductile failure. The load at initiation of FRP delamination of beams increased with the addition

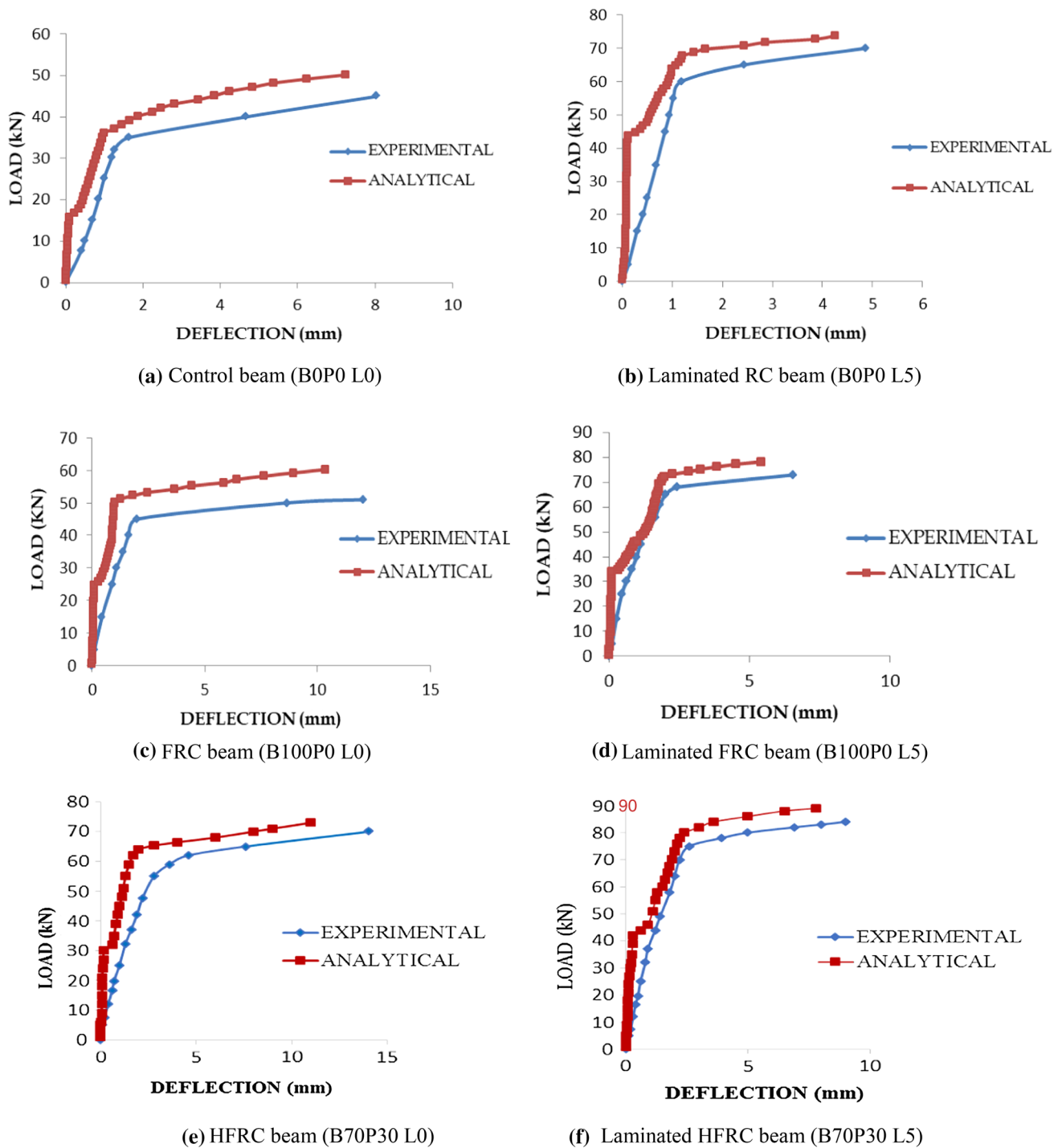


Fig. 8 a–f Load–deflection curves of all beams: experimental versus numerical

of fibres into the concrete. The ANSYS software shows circles at crushing and cracking positions. Cracking and crushing are highlighted with a circle and octahedron outline, respectively. The first crack at an integration point is shown as a red outline, whereas the second and third cracks are shown as green and blue outlines. Flexural

cracks were observed at the mid-span regions which were formed vertically up the beam. Finally, at the last load step, compression cracks appeared.

Fig. 9 Typical nodal displacement of control beam (BOP0L0) at ultimate stage

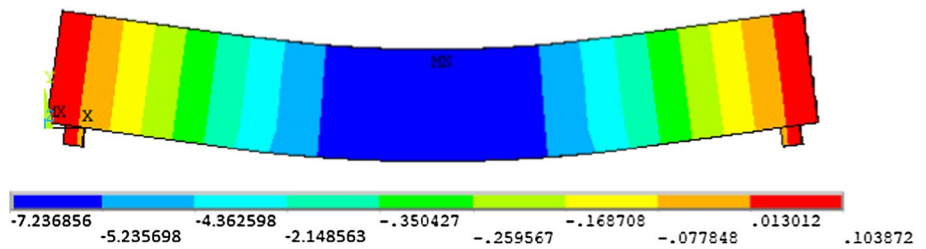
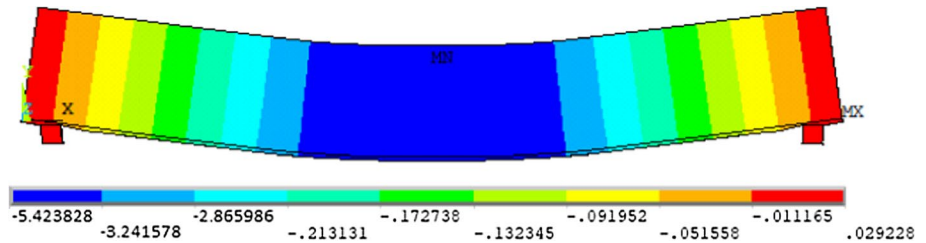
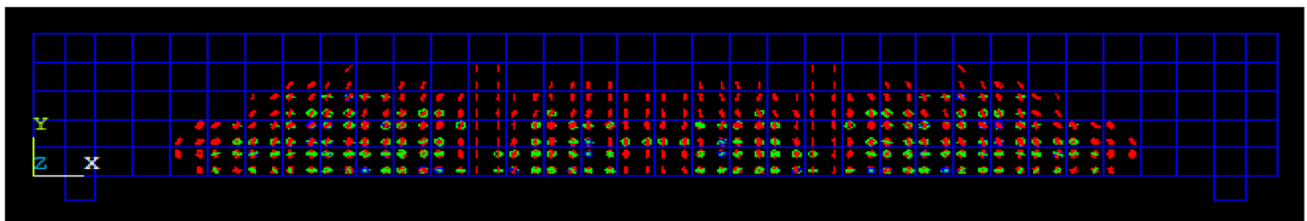


Fig. 10 Typical nodal displacement of laminated HFRC beam (B70P30L5) at ultimate stage



(a) Experimental



(b) Finite element model

Fig. 11 a–b Crack pattern of control beam (BOP0L0) at the ultimate load

Conclusions

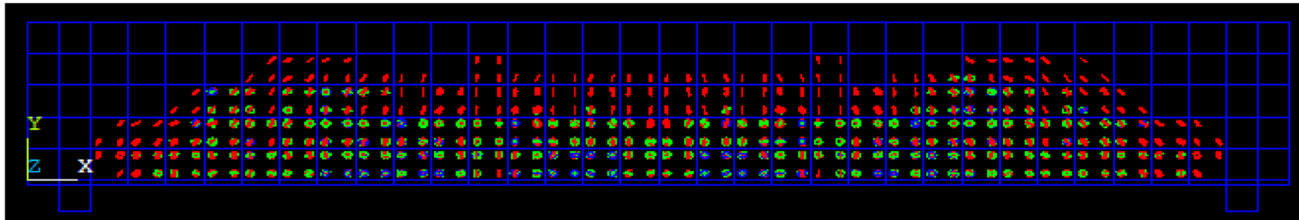
- The fibre volume fraction and combination of fibres (basalt: polyolefin) influence the load at various stages. The loads at above all stages are maximum for the laminated HFRC beam.
- The percentage enhancement in the load capacity at first crack, yield and ultimate stage of laminated HFRC beam, over the control beam, is about 79.13%, 108.82% and 81.86%. This shows that there is a combined effect of hybrid fibres and GFRP lamination.
- The deflection at ultimate load of laminated RC beam decreases over the control beam. The mid-span deflec-

tion of ‘HFRC beam’ is maximum. The percentage increase in deflection of HFRC beam over control beam is about 75.11% at the ultimate stage.

- Laminated HFRC beam has the highest ductility. The maximum increase in the deflection ductility of laminated HFRC beams ranges from 1.39 to 1.70 times the control beam and 1.59 to 1.76 times the laminated RC beam
- Yielding of steel reinforcement, followed by crushing of concrete in compression, is typical failure mode of the ‘control beam’. Failure due to debonding of laminate and rupture of laminate were typical failure modes in the case of laminated RC beam and HFRC beam, respectively.



(a) Experimental



(b) Finite element model

Fig. 12 a–b Crack pattern of laminated HFRC beam (B70P30L5) beam at the ultimate load

- The ultimate loads of all beams obtained by the FE model are slightly higher than the results from experimental study. The percentage difference between the above two methods ranges from 5 to 12%. This shows a very close agreement between the above two methods.

Acknowledgements The authors acknowledge the financial support provided by the University Grant Commission (UGC) [File No. MRP-6466/16(SERC/UGC)], New Delhi, which has immensely helped to carry out this research work successfully. The authors also wish to acknowledge the Department of Civil Engineering, Pondicherry Engineering College, Puducherry, to carry out the experimental work in the laboratories.

Compliance with ethical standards

Conflict of interest The author(s) declares that they have no conflict of interest.

References

1. American Concrete Institute (ACI) (2008) Guides for the design and construction of externally bonded FRP system for strengthening concrete structures. ACI 440.2R-08, Farmington Hills, MI
2. JSCE Japan Society of Civil Engineers (2001). Japan Concrete Engineering Series Recommendations for upgrading of concrete structures with use of continuous fibre sheets, vol141. Tokyo
3. Chiew S-P, Sun Q, Yi Yu (2007) Flexural strength of RC beams with GFRP laminates. *J Compos Constr* 11:497–506
4. Yosri AM, Ghanem GM, Mohamed AE, Salama AE (2019) Structural performance of laminated composite thin-walled beams under four-point bending. *Innov Infrastruct Solut* 4:58
5. Almomani Y, Yazdani N, Beneberu E (2020) Numerical modeling of deteriorated concrete bridge bent caps with externally bonded CFRP retrofit. *Innov Infrastruct Solut* 5:44
6. Rabinovitch O, Frostig Y (2003) Experiments and analytical comparison of RC beams strengthened with CFRP composites. *Compos B Eng* 34:663–677
7. Pannirselvam N, Nagaradjane V, Chandramouli K (2009) Strength behaviour of fibre reinforced polymer strengthened beam. *ARPN J Eng Appl Sci* 4(9):34–39
8. Hawileh RA, Rasheed HA, Abdalla JA, Al-Tamimi AK (2014) Behavior of reinforced concrete beams strengthened with externally bonded hybrid fiber reinforced polymer systems. *Mater Des* 53:972–982
9. Akbarzadeh H, Maghsoudi AA (2010) Experimental and analytical investigation of reinforced high strength concrete continuous beams strengthened with fiber reinforced polymer. *Mater Des* 31(3):1130–1147
10. Toutanji H, Zhao L, Zhang Y (2006) Flexural behavior of reinforced concrete beams externally strengthened with CFRP sheets bonded with an inorganic matrix. *Eng Struct* 28:557–566
11. Smith ST, Teng JG (2002) FRP-strengthened RC beams. I: review of debonding strength models. *Eng Struct* 24:385–395
12. Yao J, Teng JG, Lam L (2005) Experimental study on intermediate crack debonding in FRP-strengthened RC flexural members. *Adv Struct Eng* 8(4):365–396
13. Yousefieh N, Joshaghani A, Hajibandeh E, Shekarchi M (2017) Influence of fibers on drying shrinkage in restrained concrete. *Constr Build Mater* 148:833–845
14. ACI Committee 544 (1989) Measurement of Properties of Fibre Reinforced Concrete. ACI 544.2R-889, American Concrete Institute, Detroit, Michigan
15. CNR-DT204, 2006, (2007) Guide for the design and construction of fiber-reinforced concrete structures. National Research Council, Rome
16. Bawa S, Singh SP (2019) Fatigue performance of self-compacting concrete containing hybrid steel–polypropylene fibres. *Innov Infrastruct Solut* 4:57
17. Yao W, Li J, Wu K (2003) Mechanical properties of hybrid fiber-reinforced concrete at low fiber volume fraction. *Cem Concr Res* 33(1):27–30
18. Cholker AK, Tantray MA (2019) Mechanical and durability properties of self-compacting concrete reinforced with carbon fibres. *Int J Recent Technol Eng* 7(6): 1738–1743

19. Brandt AM (2009) Cement-based composites: materials, mechanical properties and performance. CRC Press, Boca Raton
20. Sahoo DR, Maran K, Kumar A (2015) Effect of steel and synthetic fibers on shear strength of RC beams without shear stirrups. *Constr Build Mater* 83:150–158
21. Dawood ET, Ramli M (2011) Mechanical properties of high strength flowing concrete with hybrid fibers. *Constr Build Mater* 28(1):193–200
22. Deak T, Czigany T (2009) Chemical composition and mechanical properties of basalt and glass fibres: a comparison. *Text Res J* 79(7):645–651
23. Branston J, Das S, Sara Y, Taylor KC (2016) Mechanical behaviour of basalt fibre reinforced concrete. *Constr Build Mater* 124:878–886
24. Li W, Xu J (2009) Mechanical properties of basalt fibre reinforced geopolymeric concrete under impact loading. *Mater Sci Eng A: Struct* 505:178–186
25. Kabay N (2014) Abrasion resistance and fracture energy of concretes with basalt fibre. *Constr Build Mater* 50:95–101
26. Jiang C, Fan K, Wu F, Chen D (2014) Experimental study on the mechanical properties and microstructure of chopped basalt fibre reinforced concrete. *Mater Design* 58:187–193
27. Alberti MG, Enfedaque A, Gálvez JC (2014) On the mechanical properties and fracture behavior of polyolefin fiber-reinforced self-compacting concrete. *Constr Build Mater* 55:274–288
28. Banthia N, Yan C (2000) Shrinkage cracking in polyolefin fiber-reinforced concrete. *ACI Mater J* 97:4
29. Eswari S, Raghunath PN, Suguna K (2008) Ductility performance of hybrid fibre reinforced concrete. *Am J Appl Sci* 5(9):1257–1262
30. El-Zohairy A, Salim H, Shaaban H, Mustafa S, El-Shihy A (2017) Experimental and FE parametric study on continuous steel-concrete composite beams strengthened with CFRP laminates. *Constr Build Mater* 157:885–898
31. Ism MM, Rabie M (2019) Flexural behaviour of continuous RC beams strengthened with externally bonded CFRP sheets. *Alex Eng J* 58:789–800
32. Chellapandian M, SuriyaPrakash S, Akanshu Sharma (2018) Experimental and finite element studies on the flexural behavior of reinforced concrete elements strengthened with hybrid FRP technique. *Comput Struct*. 208:466–478. <https://doi.org/10.1016/j.compstruct.2018.10.028>
33. Choobbor SS, Hawileh RA, Abu-Obeidah A, Abdalla JA (2019) Performance of hybrid carbon and basalt FRP sheets in strengthening concrete beams in flexure. *Comput Struct*. <https://doi.org/10.1016/j.compstruct.2019.111337>
34. IS 9103 (1999) Indian Standard concrete admixtures—specification
35. Shafiq N, Ayub T, Khan SU (2016) Investigating the performance of PVA and basalt fibre reinforced beams subjected to flexural action. *Compos Struct* 153:30–41
36. ASTM D3039 (2017) Standard Test Method for Tensile Properties of Polymer Matrix Composite Materials
37. IS 10262 (2009) Indian Standard recommended guidelines for concrete mix design. Bureau of Indian Standards, New Delhi
38. IS 456 (2000) Code of practice for plain and reinforced concrete. Bureau of Indian Standards, New Delhi
39. ICRI Guideline No. 03731—Guide for Selecting Application Methods for the Repair of Concrete Surfaces
40. Syed Ibrahim S, Eswari S, Sundararajan T (2016) Structural performance of glass fibre reinforced polymer laminated steel fibre reinforced concrete beams. *Asian J Civ Eng* 17(1):59–66
41. Ramesh B, Eswari S, Sundararajan T (2020) Flexural behavior of glass fibre reinforced polymer (GFRP) laminated hybrid-fibre reinforced concrete beams. *SN Appl Sci* 2:204
42. Ramesh B, Eswari S (2020) Structural response of GFRP strengthened hybrid fibre reinforced concrete beams. *Mater Today Oroc*. <https://doi.org/10.1016/j.matpr.2020.05.039>
43. Hassoon A, Aljanabi A (2020) Improvement of flexural capacity of hybrid, reinforced concrete spliced girders using steel fiber concrete in splice region and near surface mounted carbon fiber-reinforced polymer bars: experimental investigations. *Innov Infrastruct Solut* 5:71
44. Camata G, Spacone E, Zarnic R (2006) Experimental and non-linear finite element studies of RC beams strengthened with FRP plates. *Compos B Eng* 38:277–288
45. Attari N, Amziane S, Chemrouk M (2012) Flexural strengthening of concrete beams using CFRP, GFRP and hybrid FRP sheets. *Constr Build Mater* 37:746–757
46. Duic J, Kenno S, Das S (2018) Flexural rehabilitation and strengthening of concrete beams with BFRP composite. *J Compos Constr* 22(4):04018016
47. Hassan NZ, Sherif AG, Zamarawy AH (2015) Finite element analysis of reinforced concrete beams with opening strengthened using FRP. *Ain Shams Eng J*. <https://doi.org/10.1016/j.asej.2015.10.011>
48. Jayajothi P, Kumutha R, Vijai K (2013) Finite element analysis of FRP strengthened RC beams using Ansys. *Asian J Civ Eng (BHRC)* 14:631–642
49. ANSYS Manual (version 15)